Depot- and Diabetes-Specific Differences in Norepinephrine-Mediated Adipose Tissue Angiogenesis, Vascular Tone, Collagen Deposition and Morphology in Obesity

Lei Shen [a]*, Michael R Dashwood [b], Carlo Casale [a], Nelson N Orie [b, c], Ian M Evans [d], Pratik Sufi [e], Rosaire Gray [a, e], Vidya Mohamed-Ali [b, c]

[a]Rayne Building, University College London, London, UK,

[b]Royal Free Campus, University College London, London, UK

[c]Anti-Doping Lab Qatar, Doha, Qatar

[d]Cancer Stem Cell Team, Institute of Cancer Research, London, UK

[e]Whittington Hospital, London, UK

***Corresponding author:** Dr Lei Shen, Institute of Cardiovascular Science, University College London**,** Rayne Building, 5 University Street, London, United Kingdom. Tel: (+44)7771247328; Email: rmhalsh@ucl.ac.uk

Abstract

Aims: Norepinephrine (NE) is a known regulator of adipose tissue (AT) metabolism, angiogenesis, vasoconstriction and fibrosis. This may be through autocrine/paracrine effects on local resistance vessel function and morphology. The aims of this study were to investigate, in human subcutaneous and omental adipose tissue (SAT and OAT): NE synthesis, angiogenesis, NE-mediated arteriolar vasoconstriction, the induction of collagen gene expression and its deposition in non-diabetic versus diabetic obese subjects.

Materials and Methods: SAT and OAT from obese patients were used to investigate tissue NE content, tyrosine hydroxylase (TH) density, angiogenesis including capillary density, angiogenic capacity and angiogenic gene expression , NE-mediated arteriolar vasoconstriction and collagen deposition.

Key findings: **In the non-diabetic group**, NE concentration, TH immunoreactivity, angiogenesis and maximal vasoconstriction were significantly higher in OAT compared to SAT ($p<0.05$). However, arterioles from OAT showed lower NE sensitivity compared to SAT (10^{-8} M to $10^{-7.5}$ M, $p<0.05$). A depot-specific difference in collagen deposition was also observed, being greater in OAT than SAT. **In the diabetic group**, no significant depot-specific differences were seen in NE synthesis, angiogenesis, vasoconstriction or collagen deposition. SAT arterioles showed significantly lower sensitivity to NE (10^{-8} M to $10^{-7.5}$ M, $p<0.05$) compared to the non-diabetic group.

Significance: SAT depot in non-diabetic obese patients exhibited relatively low NE synthesis, angiogenesis, tissue fibrosis and high vasoreactivity, due to preserved NE sensitivity. The local NE synthesis in OAT and diabetes desensitizes NE-induced vasoconstriction, and may also explain the greater tissue angiogenesis and fibrosis in these depots.

Key words: adipose tissue vasculature; norepinephrine; angiogenesis; vasoconstriction; collagen; obesity

Abbreviations

ABC, Avidin Biotin Complex; BMI, body mass index; CS-GAG, sulfate-glycosaminoglycan; DAPI, 4',6-diamidino-2-phenylindole, dihydrochloride; DM, Type 2 diabetic obese patients, ECM, extracellular matrix; EGF, epidermal growth factor; fGF-2, fibroblast growth factor 2; NRP-1, neuropilin-1; FITC, fluorescein isothiocyanate; GS, griffonia simplicifolia; HDL, high density lipoprotein; HOMA, homeostasis model assessment; LDL, low density lipoprotein; NE, Norepinephrine; Non-DM, non-diabetic obese patients, OAT, omental adipose tissue; $R_{V/A}$, neovasculature to adipose tissue ratio; SAT, subcutaneous adipose tissue; TH, tyrosine hydroxylase; UEA, ulex europaeus; VEGF, vascular endothelial growth factor

1 Introduction

Abdominal obesity, consequent to expansion of both the subcutaneous (SAT) and omental (OAT) adipose tissue depots, is associated with elevated sympathetic activity [1-3]. Evidence suggests that sympathetic activity is more closely related to the deposition of OAT rather than SAT [3, 4], and that sympathetic dysfunction is further exaggerated in obese patients with Type 2 diabetes [1, 5]. A consequence of elevated sympathetic innervation and reactivity is an increase in plasma norepinephrine (NE) levels, along with elevated local NE spillover in multiple organs, including kidney and heart [6]. Recent data in rodents suggests that the AT may itself contribute to this peripheral pool of NE via the regulation on catecholamine synthesizing enzymes [7]. As NE mediates several functions of the AT, including metabolism, secretion, angiogenesis as well as vascular and tissue remodeling [8-11], changes in its levels are likely to have wide-ranging effects. Also, because sympathetic

activity is more closely related to deposition of OAT, alterations in the NE axis could differentially impact both SAT and OAT.

The angiogenic effect of NE has been mostly investigated in brown AT of rodents. NE stimulated brown adipocyte proliferation and capillary growth *in vitro* by elevating fibroblast growth factor 2 (fGF-2) mRNA and protein expression [12]. Cold exposure was associated with elevated vascular endothelial growth factor (VEGF) mRNA expression, which was abolished by sympathetic denervation but mimicked by NE administration via the β-adrenergic /cAMP/protein kinase A pathway [13-15]. However, NE-associated angiogenesis in human white AT is still under investigation.

Emerging data shows that the microvasculature embedded within the AT is directly regulated by local autocrine and paracrine signals and this is an area of much recent research activity [16]. We have previously shown NE-mediated changes in secretory function of AT [17]. NE is a classic vasoreactive molecule regulating vascular tone by binding to its functional adrenergic α and ßreceptors. It is also a potent regulator of extracellular matrix (ECM) deposition, inducing both tissue and vessel remodelling in the liver and lungs of rodents [18-21]. In humans, there is greater AT fibrosis in obese patients compared with lean individuals, and more collagen deposition surrounding vessels in OAT than SAT depots [22]. While it is probable that vascular tone is altered by the accumulation of collagens around the vessels, there is no direct evidence for this in microvessels of human AT. .

Thus, the aims of this study were to investigate, in human SAT and OAT, the depot- and diabetes-specific differences in NE production, NE-mediated angiogenesis, vasoconstriction and tissue remodelling.

2 Methods

2.1 Patient recruitment

Morbidly obese patients (N=44, 86%female) undergoing laparoscopic bariatric surgery for weight loss were recruited from the pre-operative clinic (North London Obesity Surgery Service, Whittington Hospital, London, UK). Patients with coronary artery disease, malignancy or terminal illness, connective tissue disease or other inflammatory conditions likely to affect cytokine levels, immunocompromised subjects and those with substance abuse or other causes for poor compliance were excluded. According to the clinical diagnosis, patients were separated into non-diabetic (N=28) and diabetic groups (N=16). National Ethical Committee approval was obtained for the studies and all participants provided written informed consent.

2.2 Anthropometric measurements

Body mass index (BMI) was calculated as the weight (kg) divided by the square of the height (m^2). Arterial blood pressure was measured with a digital blood pressure monitor (Datex-Ohmeda Patients Monitor, GE Healthcare, UK).

2.3 Blood and AT collection

On the day of the operation, blood samples were taken from an ante-cubital vein following an overnight fast and immediately after induction of anaesthesia. Plasma and serum samples were stored at -80 ^{o}C until further analysis.

AT from the abdominal subcutaneous and intra-abdominal greater omental depots was obtained during surgery (~5g each) and immediately transported in serum-free medium (Cellgro, Mediatech Manassas, VA) to the laboratory.

2.4 Histochemistry and immunohistochemistry

2.4.1 Estimation of catecholamine synthetic enzyme

300 mg tissue from each depot was fixed in 10% formalin for 24 hours at room temperature and then transferred to 50% ethanol at 4 ^{o}C prior to being embedded in paraffin. 3 μm sections were deparaffinised in Xylene (Sigma-Aldrich, UK) for 20 minutes, followed by dehydration in 60, 70, 80, 90, 100 % ethanol**.** AT sections were then immunostained for the catecholaminergic marker tyrosine hydroxylase (TH). Slices were washed in 0.1M PBS for 30 minutes, permeabilized and blocked with 0.1% Triton in 10% FBS for 60 minutes. Tissue was then incubated overnight at 4^{o}C in sheep anti-TH antibody (all at 1:250, Abcam, UK). Sections were washed and subsequently incubated in 488 Alexa Fluor rabbit anti-sheep antibody (1:1000) for 1 hour. Sections were cover-slipped with Vectashield HardSet mounting medium containing DAPI (Vector Laboratories, USA). The TH-stained area was isolated using the colour threshold function in ImageJ (https://imagej.nih.gov/ij/). TH-immunoreactive fibre density was calculated by measuring grey density of positive TH-stained areas with the gel analysis function. The data was expressed as arbitrary units of grey density per area.

2.4.2 Estimation of capillary density, adipocyte number and size

With the same preparation described above, the sections were also incubated for 30 minutes in a humid chamber with the staining solution containing lectin fluorescein isothiocyanate (FITC) conjugate (from Griffonia simplicifolia [GS], 25 μg/ml, Sigma-Aldrich), lectin tetramethylrhodamine isothiocyanate conjugate (from Ulex europaeus [UEA], 10 μg/ml, Sigma-Aldrich), and 4’,6-diamidino-2-phenylindole, dihydrochloride (DAPI, 0.3 μg/ml, Sigma-Aldrich). The GS lectin stains the plasmalemma, UEA stains the capillaries [23], and DAPI stains nuclei [24]. Sections were rinsed with 0.1M sodium phosphate buffer (PBS, pH 7.4) for 40 minutes and then mounted on glass slides with water-soluble mounting medium

(Cardinal Health, Dublin). Images of the stained sections were captured with a Zeiss Axioplan 2 upright microscope (Intelligent Imaging Innovations, Denver, USA) using a Photometrics CoolSnap HQ CCD camera and a Sutter Lambda LS 175W Xenon arc lamp.

Images were then analysed by ImageJ, capillaries shown as orange spots or lines were labelled and counted, and expressed as capillary number per section**.** Adipocyte number per section was counted by numbering all the adipocytes on the image. Damaged or incompletely displayed adipocytes were excluded. Adipocyte size was measured by tracing the pixel area. For tracing the pixel area, "Free Hand" function was selected in ImageJ and the border of each adipocyte was traced manually.

2.4.3 Estimation of collagen deposition

Sections were deparaffinised and rehydrated to distilled water, followed by incubation with Verhoeff's haematoxylin for 30 minutes. After washing, sections were differentiated in 2% ferric chloride solution for elastic fibre staining. Slides were then rinsed and iodine was removed. Finally, sections were counterstained in Van Giessen's for 5 minutes and then dehydrated and cover-slipped. For collagen deposition analysis, elastic fibre staining (black) was filtered using the ImageJ threshold function and the collagen staining area (pink) was measured. The data was expressed as the pixel area of collage deposition.

2.4.4 Estimation of macrophage infiltration

Slides were washed in Tris buffered saline for 2 minutes and blocked at room temperature for 5 minutes in DAKO peroxidase blocking solution and 10% horse serum. CD68 affinity purified rabbit anti-human polyclonal antibody (Sigma-Aldrich, UK) was added and incubated for 60 minutes at room temperature and secondary antibody (1 in 1000 dilution of

anti-rabbit IgG peroxidase conjugated antibody: Sigma-Aldrich, UK) for 45 min. Detection was by standard Avidin Biotin Complex (ABC)/DAB method.

2.5 Tissue culture, protein extraction and NE ELISA

50 mg of AT was minced and incubated for 24 hours in 500 µl Cellgro medium (containing 1% (v/v) penicillin/ streptomycin) at 37 ℃ in 5% CO_2. The medium was then harvested, snap-frozen in liquid nitrogen and stored at -80 ℃ until used for NE analysis. Tissue lysate was prepared with RIPA buffer (Sigma-Aldrich, UK) from ~150 mg of AT and the total protein was estimated (Novagen BCA protein Assay, EMD Chemicals, CA, USA).

NE concentrations were determined using a high sensitivity ELISA kit (Labor Diagnostika Nord GmbH & Co.KG, Germany). The concentration was expressed as NE in pg per mg of total tissue protein (pg/mg) for each sample.

2.6 NE induction of Collagen gene expression

To investigate collagen gene expression by NE, 50 mg of AT was minced and incubated for 6 hours in 500 µl Cellgro medium with 1µM NE. The tissue was stored at -80 ^{o}C prior to total RNA extraction and analysis of gene expression.

2.7 Estimation of angiogenic capacity

SAT and OAT was cut into ≈ 1 mm^3 pieces and embedded into individual wells of a 96-well plate with 50 µl growth factor reduced Matrigel (BD Bioscience, UK). Each well was then incubated with 200 µl EGM2-MV medium (Lonza, UK), and half of the medium was replaced every other day [25]. Incubation was terminated at Day10 and images were captured at 40x magnification using a Nikon TMS microscope and ProgResC14 software (resolution 1300x1030). For each sample, images were captured with five sections (whole tissue, up, down, left and right). Image information was then analysed using ImageJ. The pixel area

covered by neovasculature was traced manually and adjusted by AT area ($R_{V/A}$). Data was also analysed by particle measurement. Background of image was filtered and capillaries were isolated using the ImageJ threshold function. Then capillary quantity was estimated with the particle measurement function.

2.8 Total RNA extraction, angiogenesis microarray and real-time PCR

SAT and OAT from non-diabetic and diabetic patients was ground in liquid nitrogen. ~0.15 g AT was used for total RNA extraction by TRIzol-chlorform extraction [26].

Angiogenic gene regulation was performed using the commercially available RT^2 Profiler PCR array for human angiogenesis (PAHS-024, Qiagen, UK). The analysis and comparison of microarray data was performed automatically using Qiagen online software (https://dataanalysis.qiagen.com/pcr/arrayanalysis.php). For each gene, average value of delta Ct in each group was calculated, and the gene expression was calculated as 2^(-average delta Ct), and the fold change was calculated as the ratio of average gene expression between two groups [27].

Otherwise, cDNA was synthesized from 500 ng total RNA using a Reverse Transcription Reagent Kit (Applied Biosystems, New Jersey, USA) followed by Real-time PCR. The mRNA expression of collagen gene type Iα1 was determined with β-actin chosen as a house-keeping gene. Data was expressed as a Ct ratio of β-actin Ct/target gene.

2.9 Western Blot

Ground tissue was homogenized in RIPA buffer (Sigma-Aldrich, UK). Lysates were collected after centrifugation (3200rpm, 4^{o}C, 15 minutes), protein content measured (Novagen BCA protein Assay, EMD Chemicals, CA, USA), tissue extracts (5 μg/10 μl) loaded onto NuPAGE 4-12% Bis-Tris Gel (Novex, Life technologies, CA,USA) and

transferred to the membrane (0.45 um PVDF filter paper sandwich, Novex, Life technologies, CA,USA). Membranes were rinsed in PBS-T (Phosphate Buffer Solution + 0.1% Tween 20), blocked and incubated with antibodies to β-actin (1:1000, Sigma-Aldrich, UK) and NRP-1 (1:1000, Santa Cruz, CA, USA) at 4^{o}C overnight. Membranes were incubated with the appropriate secondary antibody (donkey anti-goat IgG, Santa Cruz, CA; or sheep anti-mouse IgG, GE Healthcare, UK) and developed using ECL Plus Western Blotting Detection System (GE Healthcare, UK). Data were expressed as the ratio of NRP-1 / β-actin grey density.

2.10 Assessment of vascular reactivity

2.10.1 Vascular tissue preparation

According to the guidelines for the measurement of vascular function and structure in isolated arteries and veins [28], small arterioles were isolated from the AT under a dissecting microscope and cut into segments (~2 mm). They were mounted on 2 wires (40 μm diameter) in an isometric myograph (500 A; DMT, Denmark) containing normal physiological salt solution (NPSS). The NPSS contained (in mM) 112 NaCl, 5 KCl, 1.8 $CaCl_2$, 1 $MgCl_2$, 25 $NaHCO_3$, 0.5 KH_2PO_3, 0.5 NaH_2PO_3, and 10 glucose (with 95% O_2/5% CO_2 to pH 7.4). Vessels were continuously aerated at 37 ℃ and pre-tensioned to an equivalent of 100 mmHg (13.3 kPa). The normalized luminal diameter of each segment was obtained as described previously [29]. An equilibration period of at least 1 hour was allowed during which time vessels were contracted with KCl (100 mM) to determine tissue viability.

2.10.2 Experimental protocol

Following equilibration, vasoconstriction was assessed by constructing cumulative concentration-response curves for NE (10^{-9} - $10^{-5.5}$ M) and the thromboxane analogue U46619 (10^{-9} - $10^{-5.5}$ M). Where possible, the dose–response curves were obtained in the

same preparation separated by a washout period of 30–60 minutes. With this protocol, there was no apparent time-dependent change in the response to any of the vasoconstrictors. Myography data were recorded and analysed using Myodaq and Myodata (Danish. Myotech, Aarhus, Denmark). In response to each dose, peak value of vessel tension was recorded; tension increase was calculated by peak value for each dose minus basal vessel tension (mN).

2.11 Assays

Plasma glucose concentration was assayed with glucose oxidase reagent (Beckman, Brea, CA, USA). Serum insulin levels were determined by ELISA (Mercodia, UK). Serum triglycerides, total, low density lipoprotein (LDL-) and high density lipoprotein (HDL-) cholesterol were assayed with commercial reagents (total-cholesterol: Boehringer-Mannhein, Sussex, UK and triglycerides: Roche Diagnostics, Herts, UK). LDL-cholesterol was calculated using the Friedwald formula [30]. All lipid assays were performed by Dr David Wickens (Chemical Pathology, Whittington Hospital, London, UK). Insulin resistance was calculated using the homeostatic model assessment (HOMA) where HOMA = (glucose in mmol/L x insulin in mIU/L)/22.5 [31]. Adipokines were measured using human 2-site ELISAs (R&D Systems, Oxon, UK) as previously described [32].

2.12 Statistical Analysis

Data were analysed using SPSS version 14 for Windows (Statistical Package for the Social Sciences, SPSS UK Ltd, Chertsey, UK). Normality of distributions was tested with the Kolmogorov-Smirnov test. Data are shown as mean (standard deviation), or for non-normally distributed data as median (interquartile range), in text and in tables. Within the same group, the comparison between SAT and OAT was done using paired non-parametric test (Wilcoxon matched-pairs test), while between non-diabetic and diabetic groups, unpaired Mann-

Whitney rank test was used. Pearson or Spearman rank correlations were used for the bivariate analysis. Significance was defined as $p \leq 0.05$.

3 Results

Patient characteristics are shown in **Table 1**. Compared to the non-diabetic group, diabetic patients were slightly older. The non-diabetic obese patients maintained normoglycaemia, but at the expense of hyperinsulinaemia. Levels of HOMA-IR, serum lipids and blood pressure were all comparable between the two groups.

Adiponectin, which is generally considered a protective adipokine, was elevated in diabetic patients, probably due to metformin therapy [33]. However serum MCP-1, a proinflammatory chemokine, was also elevated in these patients. These differences between the groups may be a consequence of medication (Medication regimen: None of the 44 patients were treated with α or ß-blockers. In the non-diabetic group only 4 out of the 28 patients were taking any medication [statins n=3 and ACE inhibitors n=1]. The diabetic patients were all treated with metformin [n=11] or diet alone. Additional medication included statins [n=6] and ACE inhibitors [n=5]).

Variables	Non-diabetic(N=28)	Diabetic(N=16)	*p* value
Gender (Male/Female)	4/24	2/14	-
Age (year)	39.9(12.3)	48.4(8.4)	0.01
BMI ($kg.m^{-2}$)	47.7(8.9)	45.0(7.8)	0.41
SBP (mmHg)	131.4(16.3)	136.4(20.1)	0.54
DBP (mmHg)	79.2(9.1)	76.4(11.8)	0.59
MABP (mmHg)	96.6(10.1)	96.4(13.6)	0.76
FPG (mmol/L)	5.1(1.0)	7.7(3.2)	<0.01
Insulin (mIU/L)	11.3(8.1-16.1)	7.1(5.7-14.4)	0.04
HOMA-IR	2.5(1.7-3.9)	2.7(1.3-5.5)	0.66
TG (mmol/L)	1.8(1.2-2.3)	1.1(0.8-2.4)	0.12
Total-chol (mmol/L)	4.2(1.2)	3.8(1.1)	0.35
LDL-chol (mmol/L)	2.6(1.3)	2.2(1.0)	0.16
HDL-chol (mmol/L)	0.9(0.2)	1.0(0.2)	0.10
Adiponectin (μg/ml)	2.53(1.61-4.48)	5.2(3.9-10.4)	<0.01
IL-6 (pg/ml)	2.14(1.48-2.60)	1.9(1.3-3.0)	0.61
MCP-1 (pg/ml)	174.4(120.4-276.6)	258.6(401.5)	0.01

Table 1 Patients' characteristics.

Data shown as mean (standard deviation) or median (interquartile range); BMI: body mass index, SBP, systolic blood pressure, DBP, diastolic blood pressure; MABP: mean arterial blood pressure; FPG, fasting plasma glucose; chol: cholesterol; TG: triglycerides; HOMA-IR, homeostasis model assessment of insulin resistance; Adiponectin, serum adiponectin; IL-6, serum interleukin-6, MCP-1, serum monocyte chemoattractant protein-1.

3.1 Tissue NE synthesis

In order to test the hypothesis that chronically elevated locally synthesized NE in the OAT and in diabetic patients may lead to vessel insensitivity to the catecholamine, the expression of the rate limiting synthetic enzyme, TH, as well as tissue and explant levels of NE were determined.

TH immunoreactivity was associated with the adipocytes, as well as with the vasculature. Lower TH density was apparent in SAT compared to OAT depots in the non-diabetic group (n=15, SAT *versus* OAT: 9.9 [7.9-12.9] *versus* 11.7 [10.0-13.9] $\times 10^4$ arbitrary unit [AU], p= 0.03, **Figure 1A & B**). However, in the diabetic patients both depots expressed equal levels of TH. When all the patients were considered together, tissue NE levels were significantly lower in SAT compared to OAT. However, when the groups were analysed separately it was only in the non-diabetic group that this depot specific difference became apparent (n=6, SAT *versus* OAT: 6.1 [0.8-563.6] versus 534.8 [2.2-2819.2] pg/mg total protein; p=0.03, **Figure 1C**), while in diabetic patients, tissue NE was comparable in the two depots (SAT *versus* OAT: 194.7 [1.4-529.7] *versus* 335.6 [6.4-3457.7] pg/mg total protein; p=0.17). Very low concentrations of NE were detected in explant medium of both SAT and OAT (0.57[0.27-0.85] and 0.28[0.22-0.5] pg/ml respectively), suggesting a mainly autocrine/paracrine, rather than an endocrine, effect.

Low levels of AT macrophage infiltration was observed in both SAT and OAT and there was no significant difference between the depots and groups, suggesting the depot-specific difference in TH is not attributed to macrophage infiltration.

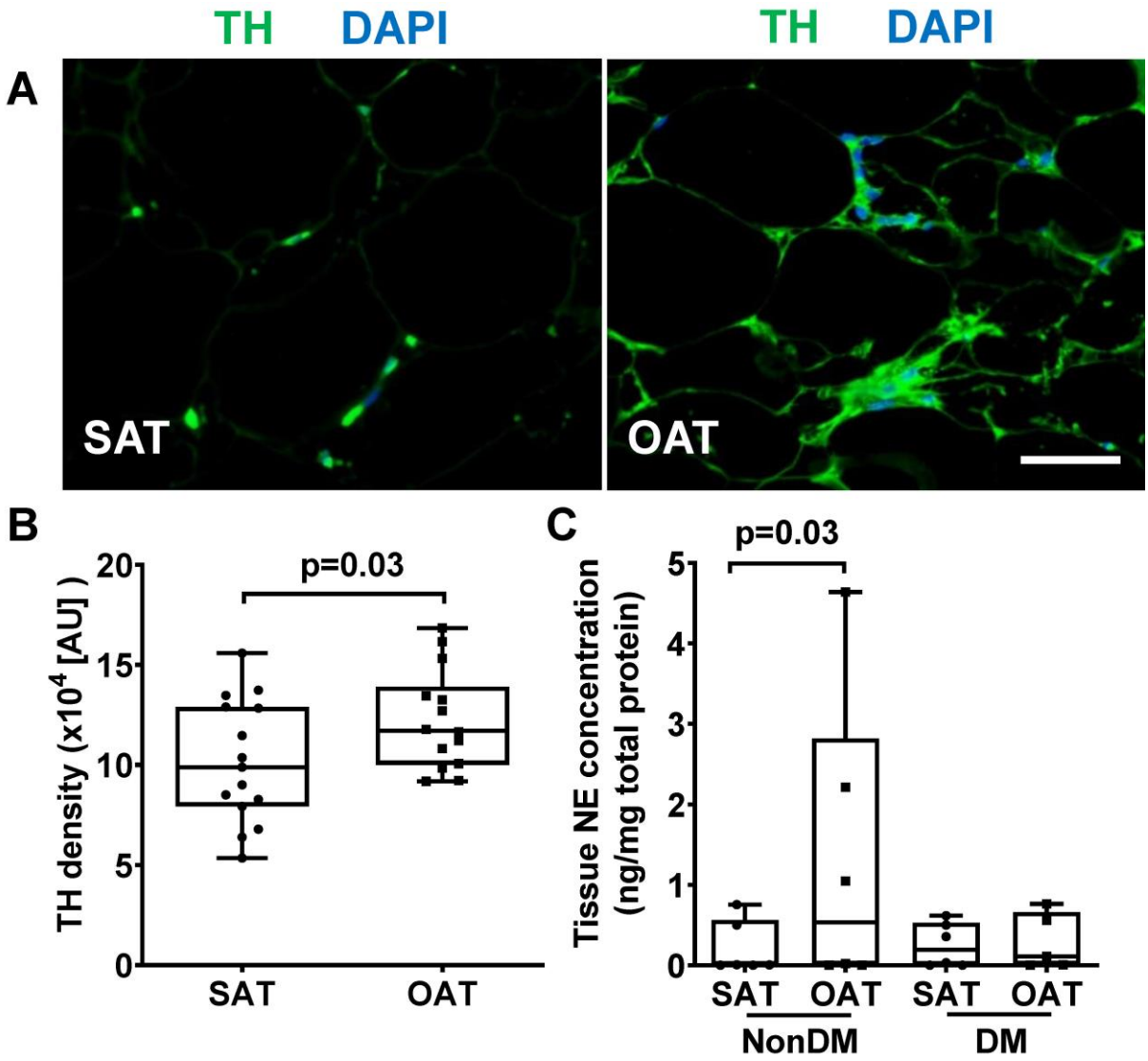

272 ***Figure 1. Depot- and diabetes-specific differences in TH density and NE levels***

273 ***(A)*** *Tyrosine hydroxylase (TH) positive staining (green) was apparent around the adipocytes*
274 *of both SAT and OAT.* ***(A&B)*** *In tissue from non-diabetic subjects TH staining was*
275 *significantly less in SAT than OAT (p=0.03). Within the diabetic group there were no*
276 *significant differences in TH staining between the depots (p=0.17).* ***(C)*** *Local NE levels were*
277 *significantly higher in OAT compared to SAT in non-diabetic while no depot-specific*
278 *difference was found in diabetes. Non-DM: non-diabetic obese patients; DM: Type 2 diabetic*
279 *obese patients; Scale: 100 μm*

280 **3.2 Depot- and diabetes-specific differences in AT angiogenesis**

3.2.1 Capillary density and angiogenic capacity

As displayed in **Figure 2A**, in the non-diabetic group, SAT showed a significantly lower capillary number compared to OAT (p=0.01), while in the diabetic patients, no significant depot-specific difference was observed. Furthermore, capillary numbers were greater in SAT of diabetic, compared to non-diabetic, patients (p=0.05). This finding was confirmed by manually counting the capillary numbers in each section (**Figure 2B)**. Moreover, the capillary density was calculated as the number of vessels per adipocyte, the depot-specific difference remains significant in non-diabetic group (n=7, SAT: 0.67 [0.63-0.77] *versus* OAT: 0.87[0.67-1.06], **Figure 2C**)

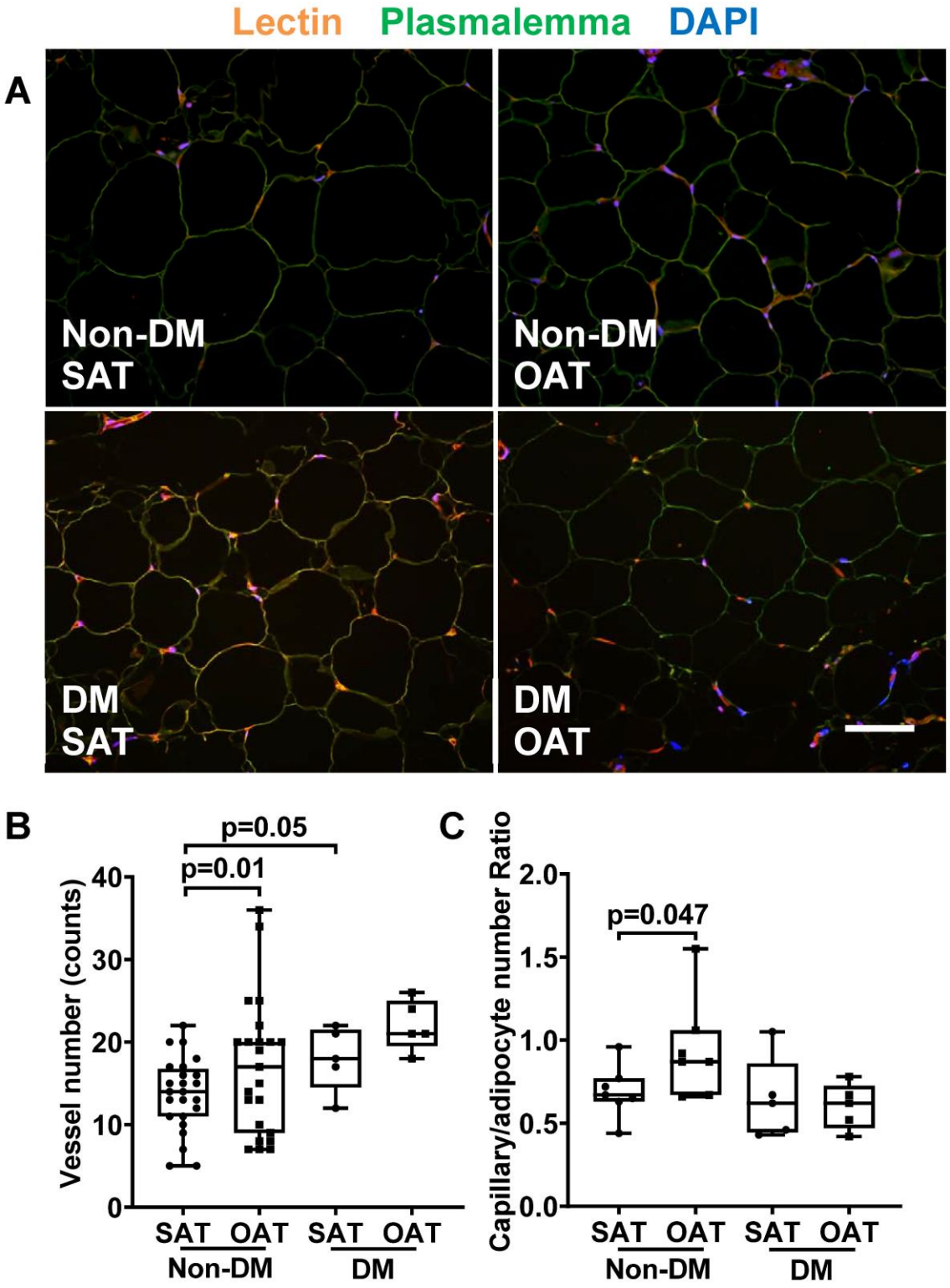

290 ***Figure 2. Depot- and diabetes-specific differences in AT angiogenesis***

291 ***(A)*** *Capillary density is significantly lower in SAT than OAT in non-diabetic group, while no*

292 *significant depot-specific difference was observed in diabetic group, SAT and OAT showed*

elevated but comparable numbers of capillaries. ***(B)*** *Nonparametric comparison showed SAT in non-diabetic group has the lowest numbers of capillaries compared to OAT and diabetics.* ***(C)*** *The depot-specific difference of capillaries remained significant after calibrating to adipocyte number. Scale: 100 μm.*

Angiogenic capacity was also significantly different between the depots in the non-diabetic group, with greater neovasculature in OAT compared to SAT (n=12, $R_{V/A}$ SAT: 8.5[8.0-9.5] *versus* OAT: 12.9[8.4-18.9], p=0.03, **Figure 3A top panel &B**). However, no significant depot-specific difference of angiogenic capacity was detected in the diabetic group (**Figure 3A bottom panel &B)**. The angiogenic capacity of the SAT of diabetics was higher compared to that of non-diabetics ($R_{V/A}$ non-diabetic SAT: 8.5[8.0-9.5] versus diabetic SAT: 11.5[10.8-11.4], p=0.004, **Figure 3B**).

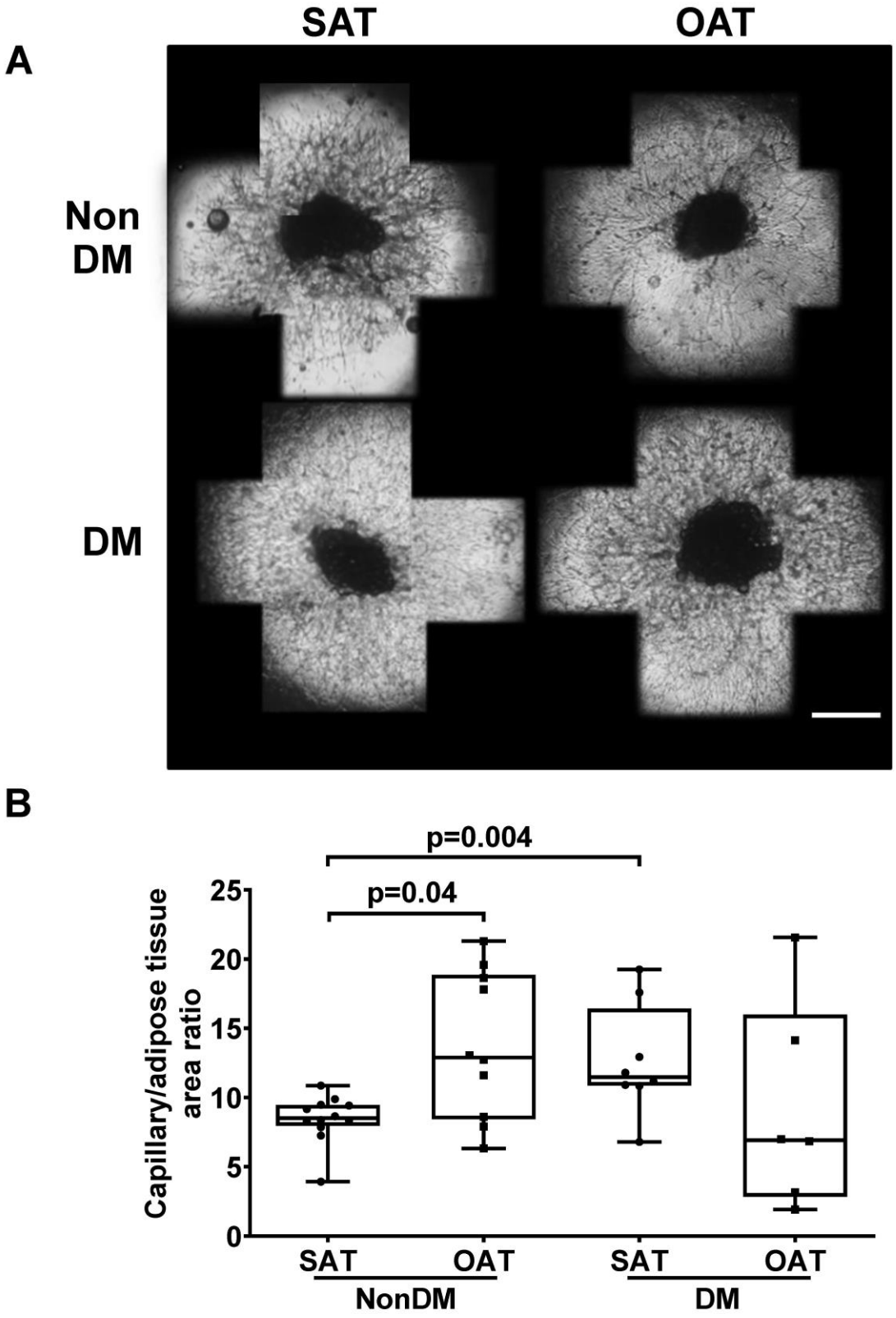

304 ***Figure 3. Depot- and diabetes-specific differences in AT neovascular sprouting***

(A) *In the non-diabetic group, less neovasculature expansion was seen in SAT compared to OAT. In the diabetic group, no significant depot-specific difference was observed in SAT compared to OAT. Furthermore, SAT in the diabetic group showed significantly higher angiogenic capacity compared to SAT in the non-diabetic group.* ***(B)*** *This finding was confirmed by nonparametric test on neovasculature to adipose tissue area ratio ($R_{v/a}$) showing that SAT in the non-diabetic group showed the lowest angiogenesis compared to OAT and diabetics. Scale: 1mm.*

3.2.2 Depot- and diabetes-specific expression of genes regulating angiogenesis

Given the observed depot- and diabetes-specific differences in capillary density, we investigated the expression of genes considered essential for angiogenesis using a pathway specific array. In the non-diabetic tissue, of the 84 genes on the array, 11 were up-regulated while 5 were down-regulated by > 2-fold in OAT compared to SAT. However, in the diabetic patients, only 7 out of these 11 genes were up-regulated and 9 were down-regulated in the OAT compared to SAT (**Figure 4A**).

Assessment of the effect of diabetes on gene expression in the two depots showed a greater number of genes upregulated in the SAT of diabetic, compared to the non-diabetic tissue (**Figure 4B**), especially those of epidermal growth factor (EGF) and neuropilin-1 (NRP-1). However, in the OAT only 4 genes, mainly chemokines/cytokines, were upregulated in the diabetic, compared to the non-diabetic tissue, while 3 others were lower in the OAT of diabetics compared to the non-diabetics (**Figure 4B**). To further validate the accuracy of the angiogenesis microarray, NRP-1, a potent mediator of angiogenesis showing the greatest alteration amongst the genes modulated by diabetes in the SAT, was investigated at the protein level. A depot-specific difference was identified with NRP-1 more highly expressed in OAT compared to SAT in non-diabetic group (**Supplement Figure 1**).

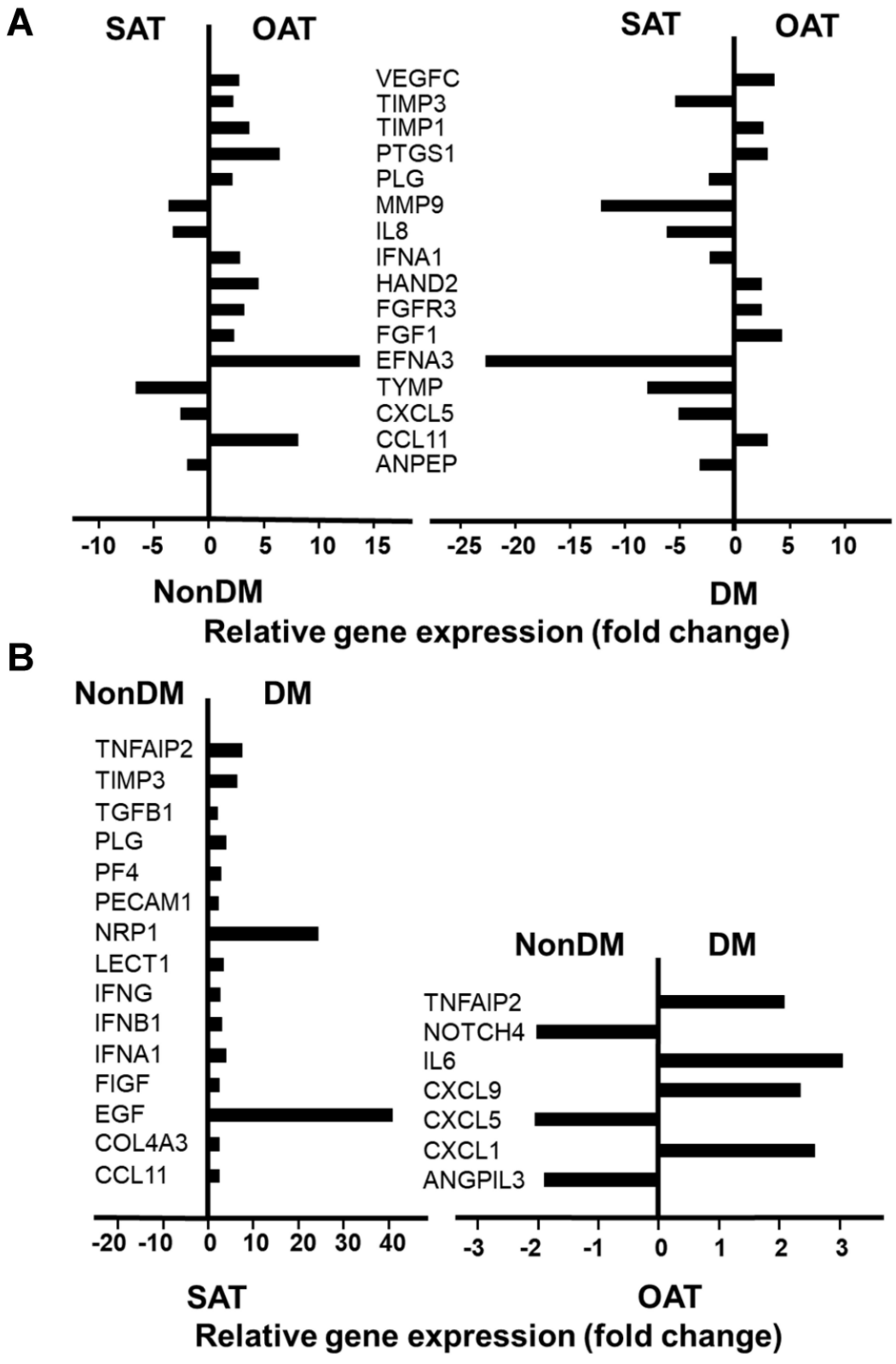

329 ***Figure 4. Depot- and diabetes-specific differences in AT angiogenesis-related gene***

330 ***expression***

(A) *In the non-diabetic group, most angiogenic genes were up-regulated in OAT (n=11) compared to SAT (n=5), while diabetic patients showed comparable numbers of gene expression in SAT (n=9) and OAT (n=7).* ***(B)*** *In the comparison between the non-diabetic and diabetic group, all gene expression was up-regulated in SAT in diabetes, while no significant diabetes-specific difference was found in OAT. VEGFC: vascular endothelial growth factor C; TIMP: TIMP metallopeptidase inhibitor; PTGS1: prostaglandin-endoperoxide synthase 1; PLG: plasminogen; MMP9: matrix metallopeptidase 9; IFNA1: interferon, alpha 1; HAND2: heart and neural crest derivatives expressed 2; FGFR3: fibroblast growth factor receptor 3; FGF1: fibroblast growth factor 1 (acidic); EFNA3: ephrin-A3; TYMP: thymidine phosphorylase; CXCL: chemokine (C-X-C motif) ligand; CCL: chemokine (C-C motif) ligand; ANPEP: alanyl (membrane) aminopeptidase; TNFAIP2: tumor necrosis factor, alpha-induced protein 2; TGFB1: transforming growth factor, beta 1; PF4: platelet factor 4; PECAM1: platelet/endothelial cell adhesion molecule; LECT1: leukocyte cell derived chemotaxin 1; IFNG: interferon, gamma; IFNB1: interferon, beta 1, fibroblast; IFNA1: interferon, alpha 1; FIGF: C-fos induced growth factor (vascular endothelial growth factor D); EGF: epidermal growth factor; COL4A3: collagen, type IV, alpha 3; NOTCH4: notch 4; ANGPIL3: angiopoietin-like 3.*

3.3 NE-mediated vasoconstriction

In all subjects the vasocontractile function of arterioles with comparable lumen sizes were investigated (non-diabetics: SAT *versus* OAT: 306.9 [215.9-440.0] *versus* 335.1 [233.4-430.4] μm, p=0.73, n=16; diabetics: SAT *versus* OAT: 278.8 [179.4-442.5] *versus* 330.8 [181.1-592.8] μm, p=0.72, n=10).

In the non-diabetic group, there was a significant depot specific difference in both the sensitivity to NE mediated vasoconstriction and the maximal contractile response. The

arterioles from the SAT showed vasoconstriction at lower, near physiological doses of NE (at dose 10^{-8} M, p=0.01; dose $10^{-7.5}$ M, p=0.02; Log EC_{50}: SAT versus OAT, -7.3[0.6] versus -6.2[0.6], **Figure 5A & B**). However, the maximal contractile response of the OAT vessels was higher compared to SAT vessels (SAT *versus* OAT: 3.65 [1.90-6.75] *versus* 8.03 [4.07-10.88] mN, p=0.05, **Figure 5A & B**).

No depot specific differences in the sensitivity or vessel tension were seen in the diabetic group (SAT versus OAT maximal vessel tension, p=0.83, Log EC_{50}: SAT versus OAT, -6.4[0.7] versus -6.4[0.8], **Figure 5A & C**).

3.4 Thromboxane (U44419)-mediated vasoconstriction

To examine if other vasoconstrictors also elicited a similar depot specific difference in response, U46619, a thromboxane mimic and a powerful vasoconstrictor, was tested in the non-diabetic group. No difference in sensitivity to U46619-mediated vasoconstriction was apparent between SAT and OAT derived arterioles (**Figure 5D**, Log EC_{50}: SAT versus OAT, -6.3[1.0] versus -6.8[0.7], p=0.29, n=9). However, at supra-pharmacological doses OAT arterioles exhibited greater vasoconstriction (10^{-6}-$10^{-5.5}$M, p=0.02).

Furthermore, in the comparison between thromboxane- and NE-mediated vasoconstriction in the non-diabetic group, the vessel tensions mediated by thromboxane were significantly lower compared to those mediated by NE in SAT (10^{-8} M to $10^{-6.5}$ M, $p<0.05$, **Figure 5E**), while there were no such differences detected in OAT, which suggests a NE-specific vessel sensitivity in SAT of non-diabetic patients.

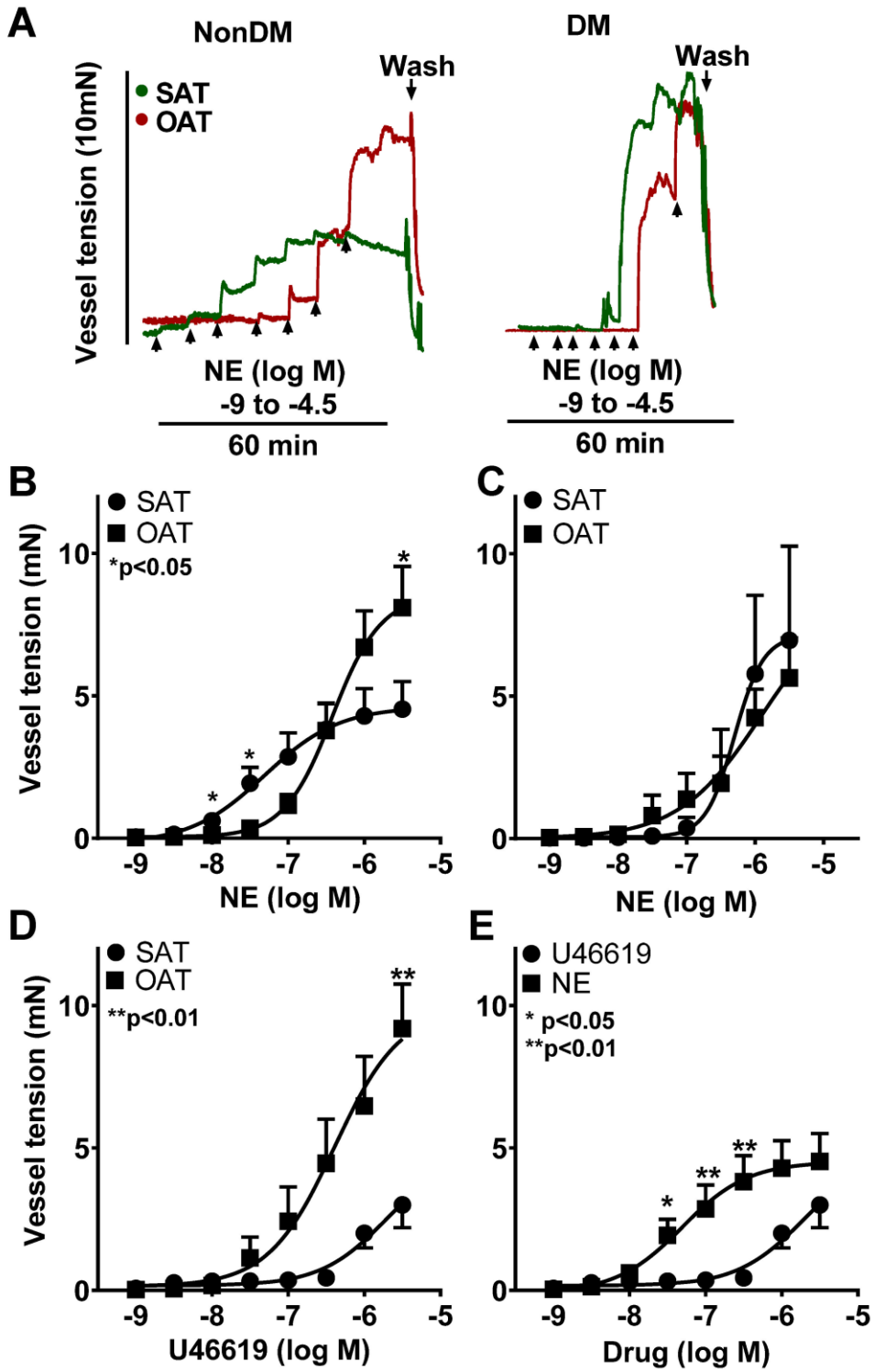

375 ***Figure 5. Depot- and diabetes-specific differences in NE mediated vasoconstriction***

376 ***(A)*** *Trace readings showed a depot-specific difference in vasoconstriction of the non-diabetic*

377 *group, which was abolished in diabetic patients.* ***(B)*** *In the non-diabetic group, SAT,*

378 *compared with OAT, arteriole showed greater sensitivity to NE-induced vasoconstriction (10*

^{8}-$10^{-7.5}$ M, $p<0.05$, Log EC_{50}: SAT versus OAT, -7.3[0.6] versus -6.2[0.6]) but lower maximal tension (SAT versus OAT, $p=0.02$). ***(C)*** *However, the NE sensitivity and maximal tension differences were abolished in the diabetic group, which is mainly caused by blunted vasoconstriction in SAT (Log EC_{50}: SAT versus OAT, -6.4[0.7] versus -6.4[0.8]).* ***(D)*** *No significant sensitivity difference was found in thromboxane analogue U46619 –mediated vasoconstriction between SAT and OAT in the non-diabetic group, which suggests a NE-specific change of vessel sensitivity in SAT.* ***(E)*** *NE mediated vasoconstriction was significantly higher compared to that mediated by U46619 in SAT of the non-diabetic group (10^{-8} M to $10^{-6.5}$ M, $p<0.05$).*

3.5 Collagen deposition and gene expression, and NE-mediated AT fibrosis

As shown in **Figure 6A**, in SAT of the non-diabetic group, low levels of collagen deposition was observed surrounding the vessels and dispersed within the rest of the tissue, while OAT showed significantly higher collagen staining which was mostly near the vessels, but, also throughout the tissue. Greater fibrosis was observed in all the diabetic tissues. In SAT, collagen staining was observed around the vessels and widely dispersed within the tissue, suggesting tissue fibrosis and perhaps consequent vessel stiffness. Similar results were also found in OAT of this group. This finding was confirmed by collagen pixel area analysis and gene expression data. SAT of non-diabetic subjects displayed the lowest collagen deposition compared to OAT of the non-diabetic group and both depots of the diabetic group (Non-diabetic group: n=16, diabetic group: n=15, $p<0.05$, **Figure 6B**).

Collagen gene type Iα1 expression also showed the same trend, with SAT of non-diabetic patients having the lowest mRNA gene expression compared to OAT in the non-diabetic group and both depots in the diabetic group (n=15, **Figure 6C**).

Significant elevation of collagen type Iα1 mRNA expression was observed in AT incubated with 1μM NE, compared with the control [NE: 0.67(0.64-0.68) versus Control: 0.62(0.61-0.65), n=6, p=0.03], which implicates NE directly in AT remodeling.

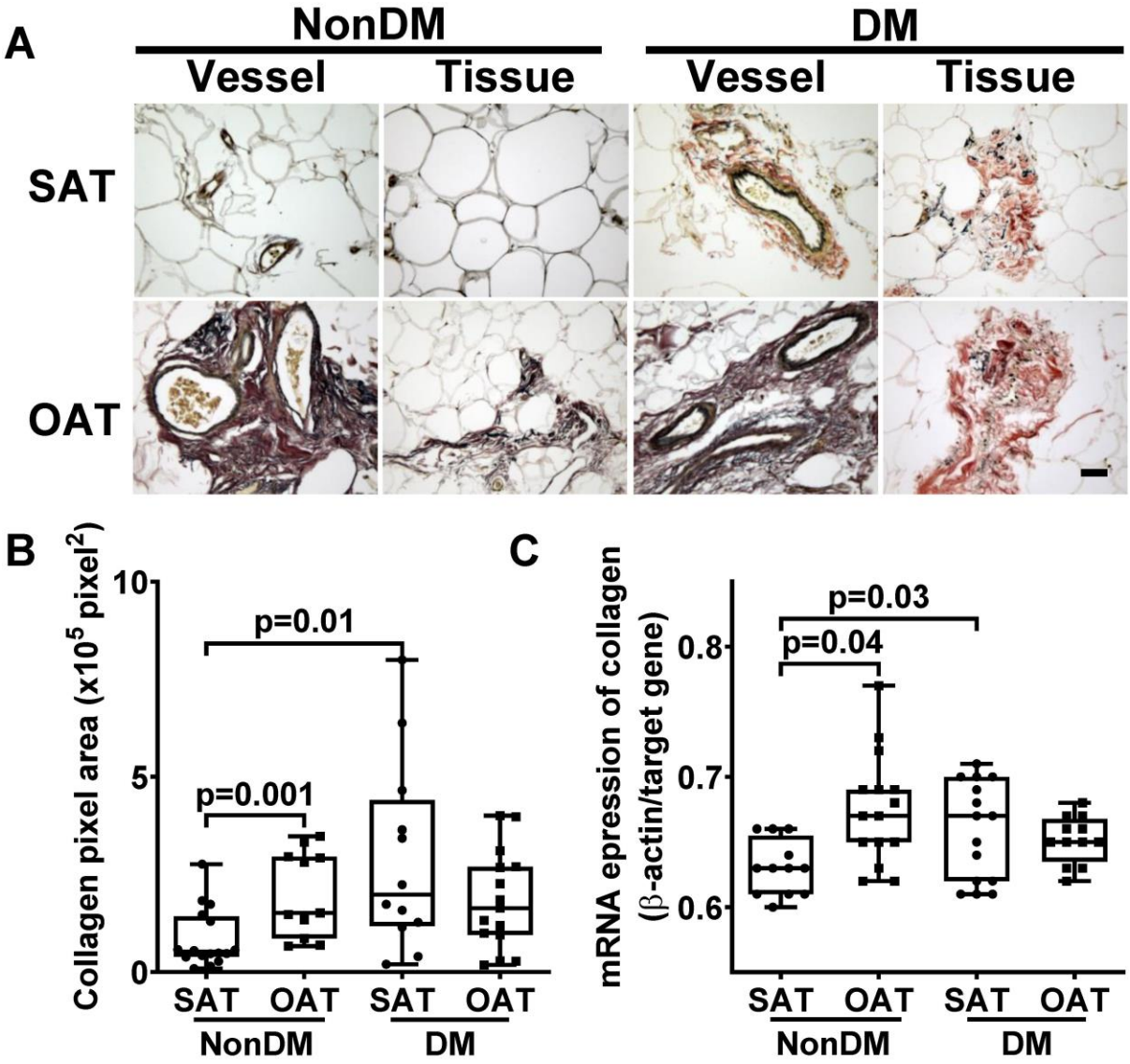

Figure 6. Depot- and diabetes-specific differences in collagen deposition and collagen expression.

(A) *Collagen was stained as pink and elastin was stained as black. Representative images were selected to show the collagen deposition surrounding the vessels and within the area of the rest of the tissue.* ***In the non-diabetic group****, SAT showed little collagen staining both within the vessel area and the surrounding region, while abundant collagen deposition was*

shown in OAT wrapping the vessel. Also there was clear collagen staining in the rest of the tissue. ***In the diabetic group****, more collagen deposition was observed compared to the non-diabetic group. In SAT, collagen was not only around the vessels but also widely dispersed within the tissue. OAT showed a similar collagen distribution and comparable collagen quantity. Scale: 100μm.* ***(B)*** *Collagen staining analysis showed the least collagen deposition in SAT of non-diabetic patients compared to OAT of non-diabetics and both depots in diabetes.* ***(C)*** *The same trend has also been shown in collagen gene Type Iα1 expression.*

3.6 Adipocyte size

Adipocyte size was assessed by calculating the pixel area. In the non-diabetic subjects OAT, compared to SAT, showed significantly smaller adipocytes (SAT: adipocyte number=260, 1.5[1.0-2.1] $x10^4$ μm^2, OAT: adipocyte number= 286, 1.2[0.8-1.7] $x10^4 \mu m^2$, $p<0.0001$). The SAT depot of diabetic patients had larger adipocytes compared to those of non-diabetic patients (diabetic *versus* non-diabetic SAT: 1.7 [1.1-2.5] $x10^4 \mu m^2$ *versus* 1.5[1.0-2.1] $x10^4$ μm^2, p=0.04). However, in the OAT these differences were not significant (diabetic *versus* non-diabetic OAT: 1.2 [0.7-1.7] $x10^4$ μm^2 *versus* 1.2[0.8-1.7] $x10^4$ μm^2, p=0.9). Furthermore, the largest adipocytes were found most frequently in the diabetic depots (**Figure 7**).

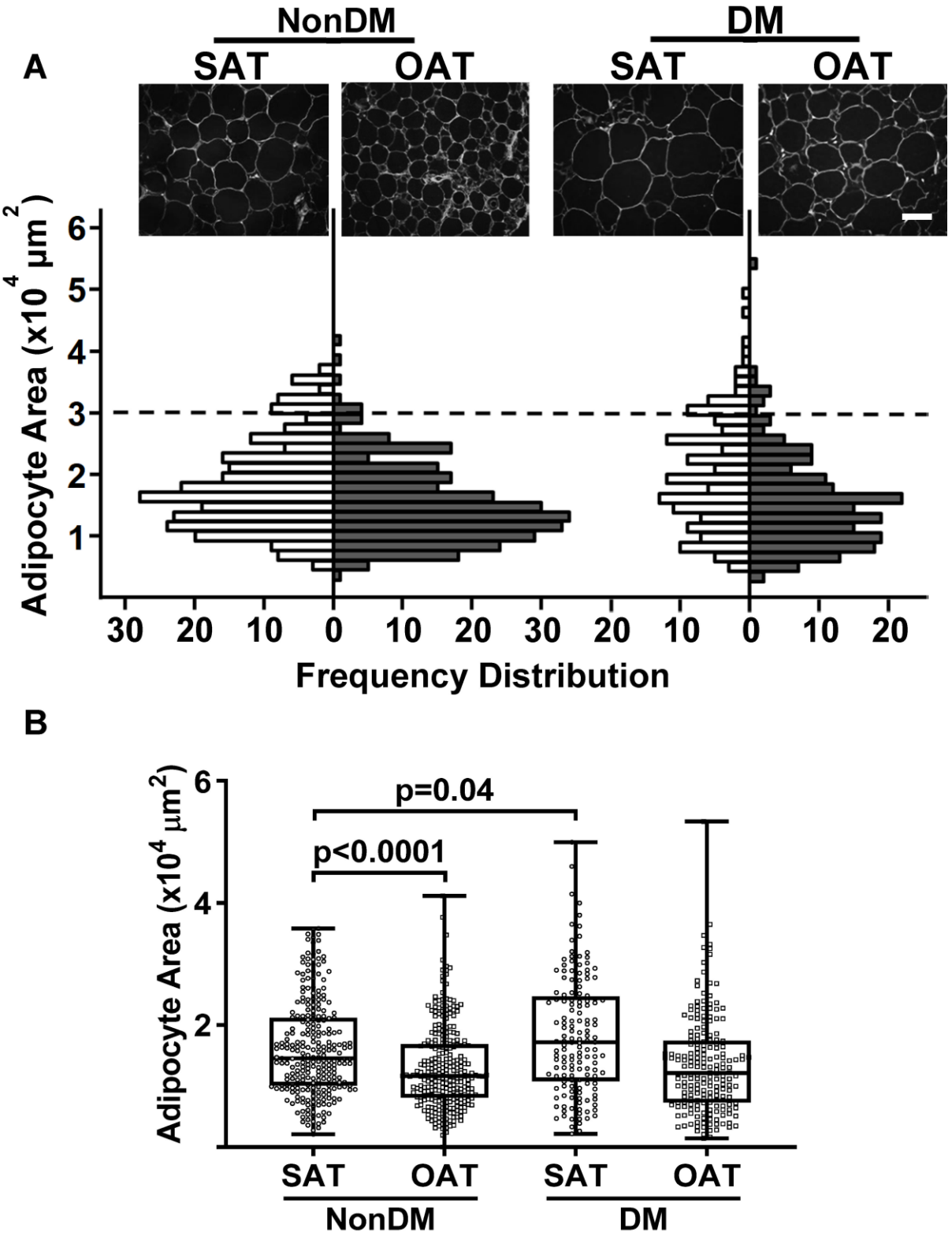

427 ***Figure 7. Depot- and diabetes-specific differences in adipocyte size***

428 *(A) A greater number of the smaller adipocytes were observed in OAT compared to SAT in*

429 *both groups, while SAT and OAT of diabetic patients displayed more large adipocytes*

compared to those in the non-diabetic group (upon the dotted line). (B) ***In non-diabetic group****, adipocyte size was significantly larger in SAT compared to OAT (p<0.0001);* ***In diabetic group,*** *adipocytes of SAT showed to be significantly larger than those of non-diabetic group (p=0.04), which suggests tissue hypertrophy. Scale: 100μm*

4 Discussion

There are several key and novel findings in this study. Firstly, depot- and diabetes-specific differences of the NE synthesis by human white AT has been observed, with levels being the lowest in the SAT of non-diabetic obese patients. Secondly, this depot also showed less angiogenesis, including lower capillary staining, neovascular sprouting and the expression of angiogenic genes. Thirdly, the arterioles from the SAT of non-diabetic patients also showed higher sensitivity to NE-mediated vasoconstriction, at levels near physiological doses. However, all other depots (OAT of non-diabetics and both SAT and OAT of diabetics) showed lower sensitivity to NE. This difference between depots in sensitivity to vasoconstriction was specific to NE, as thromboxane (U46619)-mediated vasoconstriction was comparable in vessels from SAT and OAT. Fourthly, the SAT depot of the non-diabetic patients also exhibited less collagen deposition, with lower expression of the collagen genes, perhaps a consequence of low NE synthesis locally, as NE directly induced collagen mRNA expression. Finally, the frequency of the largest adipocytes are greater in both the SAT and OAT of the diabetic, compared to the non-diabetic, patients. Perhaps this infers greater necrosis-prone cells in these depots compared to SAT of non-diabetics. Overall these data showed significant depot-specific differences in NE synthesis, NE-associated angiogenesis, vasoconstriction, and collagen deposition in non-diabetic obese individuals. In contrast there was an absence of such differences in patients with diabetes.

4.1 Local NE synthesis in AT

TH, a key enzyme involved in NE synthesis, was found in both depots, but greatly elevated in OAT compared to SAT, specifically around the adipocytes, confirming not only the ability of these depots to synthesize this hormone but also the differences in their ability to express this enzyme. However, the cellular origin of the enzyme i.e. whether from sympathetic nerve endings or derived from any other cellular sources within the AT was not clear. Adipocytes from rodents were shown to synthesize catecholamine as a consequence of stress-related immune response [34-36] and AT macrophages have been shown to produce NE, particularly in response to cold stress [37, 38]. A very recent study also suggests that macrophages and adipocytes could co-regulate the expression of NE synthetic enzymes [39]. Since no differences in macrophage infiltration (determined by CD68 staining) between the depots were found, these cells are unlikely to have contributed significantly to the observed differences in NE synthesis between OAT and SAT in this study. Furthermore, NE was detected in protein extracts from whole AT but not in explant medium suggesting a more localized accumulation, with the potential to impact the embedded microvasculature.

4.2 Paradox between high angiogenesis and inflammation/hypoxia in OAT and diabetes

AT angiogenesis has been shown to be beneficial in rodents, with sufficient angiogenesis being able to prevent tissue hypoxia and reverse insulin resistance [40, 41], while it has been reported recently that vascular formation of SAT was inhibited in obesity through TWIST1-SLIT2 signalling [42]. In this study, non-diabetic obese patients showed greater capillary numbers and angiogenic capacity in OAT. Also, most of the angiogenic genes were upregulated in OAT compared to SAT. Despite this, the OAT displayed a more inflammatory and hypoxic micro-environment [43-45], which perhaps indicates that increased capillary density and angiogenesis are not sufficient to counter the local AT hypoxia. This could be attributed to the dysfunction in vascular tone, since convincing data demonstrated that the vasodilation was impaired in OAT but preserved in SAT [46-48]. Additionally, current data

suggests vasoconstriction was also compromised, perhaps due to the NE desensitization. Another recent *in vivo* study found that blood flow of brachial artery was 1.6-fold lower in obese patients compared to lean controls, which was significantly correlated with OAT volume [49]. Therefore, vascular tone dysfunction may directly restrict local AT blood flow and contribute to the local hypoxic environment. Furthermore, there was also an elevation of capillary numbers and angiogenic capacity in SAT of diabetic compared to non-diabetic subjects. The effect of hyperglycemia and diabetes on angiogenesis is conflicting. In retinopathy, nephropathy, and atherosclerotic plaque, there was excessive angiogenesis, while the neovascularisation was decreased in wound healing and myocardial perfusion [50]. In this study, SAT in the diabetic group was more angiogenic compared to that of non-diabetics, and the microarray data suggests this increase, besides its association with sympathetic overreaction, could be also caused by the elevation of a series of angiogenic factors.

4.3 NE-mediated vasoconstriction and vascular desensitization

Consistent with higher tissue NE levels, OAT vessels displayed reduced sensitivity to this catecholamine compared to SAT vessels from non-diabetic obese subjects, a finding supported by the recent study showing the impaired vasoreactivity mediated by β-adrenoceptors in visceral AT of mice on high fat diet [48]. Although the mechanism is unclear, prolonged exposure to high NE could lead to the desensitization of receptor-G protein coupling domain in response to adrenergic receptor stimulation [51]. In different tissue and cells, desensitization of G-protein-coupled receptors (GPCRs) could occur via GPCR-kinase / β-arrestin pathway [52, 53]. This differential sensitivity to NE was absent in arterioles from obese diabetic subjects in line with the comparable high NE synthesis in both depots and the relative reduction in sensitivity compared with SAT from the non-diabetic obese subjects. This is consistent with the significant increase in microvascular volume observed in non-diabetic compared to the diabetic group following intravenous adrenaline

infusion [54]. This could also be explained by the NE desensitization in SAT arterioles of diabetic patients, while the response to the thromboxane analogue U46619 was unaffected in these circumstances, suggesting specific alteration of noradrenergic mechanism in obesity/diabetes. What was clearly not affected in both the non-diabetic and diabetic groups is the higher maximum contractile force generated by OAT vessels compared to SAT vessels. This may simply be a reflection of an inherently greater capacity of OAT vessels to generate more force compared to the SAT vessels and which was unaffected by obesity or diabetes. The maximum contractile force appears to be dissociated from the sensitivity to NE in human AT vessels in obesity/diabetes. The coexistence of dampened vascular sensitivity to NE and endothelial dysfunction (commonly associated with both obesity and diabetes [55-57]) may have a negative impact on local blood flow and tissue metabolism and perpetuate insulin resistance.

4.4 NE-mediated AT fibrosis and its effect on vasoreactivity and adipocyte morphology

Increased tissue stiffness in visceral AT has been reported recently in mice on a high fat diet [48]. Our current study also showed an upregulation of collagen mRNA and collagen deposition in OAT of non-diabetics and in both SAT and OAT of the diabetic group. Again, this may, at least in part, be driven by an increase in NE synthesis in these depots since incubation with NE demonstrably increased collagen mRNA expression in these tissues. Moreover, NE has been shown to increase fibrotic responses in several organs and vessels [20, 21, 58, 59]. An increase in collagen deposition within and around blood vessels in AT in obese or obese diabetic individuals would increase resistance to blood flow and further exacerbate tissue hypoxia, inflammation and necrosis. Furthermore, the mechanical stress associated with increased collagen deposition might also impact on adipocyte size. Although current data is not adequate to identify the specific subtypes of collagen seen in this study, collagen gene Type Iα1 was detected and was also up-regulated by NE incubation. In both rat

and human, the imbalance between collagen Type I deposition and degradation is associated with myocardial fibrosis and essential hypertension [60, 61]. The likelihood of a similar effect on AT vascular function in obesity/diabetes is supported by the current data.

5 Conclusion

The interaction between the vasculature and AT is crucial in maintaining AT normal function and remodelling capacity. Preserved vascular NE sensitivity as well as low levels of local AT NE synthesis may play a key role to protect AT from tissue fibrosis, inflammation and hypoxia. This study has demonstrated that local NE spillover of AT desensitized adrenergic regulation of vasoconstriction, meanwhile vessel stiffness was increased due to elevating tissue fibrosis, perhaps consequently leading to a vascular hyporeactivity, which may be associated with AT dysfunction. Concomitantly, angiogenesis was triggered, perhaps to compensate for the compromised vascular function, as observed in OAT and diabetes. Due to the vascular dysfunction, neovascularization, even at relatively normal or high levels, may not be adequate to reverse local hypoxia and inflammation but only facilitate the 'unhealthy' tissue expansion.

6 Acknowledgements

Great thanks to Miss Stefania Simou, MSc in Clinical and Public Health Nutrition, University College London, for capturing the Matrigel images and performing the initial data analysis, and to all patients and volunteers for their kind support in this study.

7 Funding

This work was supported by the European Commission integrated project (LSHM-CT-2004-005272/ exgenesis) and Whittington Hospital translational research small grants scheme.

8 Conflict of Interest

None

9 Authors' contributions

LS collected and processed the samples, performed most experiments and data analysis, prepared and revised this manuscript. MRD provided valuable comments and strong support throughout the preparation and revision of this manuscript. CC collected and processed the samples, performed experiments including RNA extraction, ELISA and analysed macrophage staining data. NNO provided technical support and generated the preliminary data in myography study, and revised the manuscript. IME provided technical support in most studies and revised the manuscript. PS and RG provided clinical support and helped consenting patients and collecting blood and adipose tissue samples during surgeries. VM developed the research hypothesis, designed the study, supervised most research works and revised the manuscript. All authors have approved the manuscript.

10 References

[1] N.E. Straznicky, M.T. Grima, C.I. Sari, N. Eikelis, E.A. Lambert, P.J. Nestel, M.D. Esler, J.B. Dixon, R. Chopra, A.J. Tilbrook, M.P. Schlaich, G.W. Lambert, Neuroadrenergic dysfunction along the diabetes continuum: a comparative study in obese metabolic syndrome subjects, Diabetes 61(10) (2012) 2506-2516.

[2] G. Grassi, A. Biffi, G. Seravalle, F.Q. Trevano, R. Dell'Oro, G. Corrao, G. Mancia, Sympathetic neural overdrive in the obese and overweight state, Hypertension 74(2) (2019) 349-358.

[3] G.E. Alvarez, S.D. Beske, T.P. Ballard, K.P. Davy, Sympathetic neural activation in visceral obesity, Circulation 106(20) (2002) 2533-2536.

[4] M.L. Garcia, M.I.O. Milanez, E.E. Nishi, A.Y.S. Sato, P.M. Carvalho, F.N. Nogueira, R.R. Campos, L.M. Oyama, C.T. Bergamaschi, Retroperitoneal adipose tissue denervation

improves cardiometabolic and autonomic dysfunction in a high fat diet model, Life Sci 283 (2021) 119841.

[5] G. Jia, J.R. Sowers, Hypertension in diabetes: an update of basic mechanisms and clinical disease, Hypertension 78(5) (2021) 1197-1205.

[6] M. Esler, G. Lambert, G. Jennings, Regional norepinephrine turnover in human hypertension, Clin Exp Hypertens 11 Suppl 1 (1989) 75-89.

[7] A. Gomes, R. Soares, R. Costa, F. Marino, M. Cosentino, M.M. Malagon, L. Ribeiro, High-fat diet promotes adrenaline production by visceral adipocytes, Eur J Nutr 59(3) (2020) 1105-1114.

[8] S.Y. Park, J.H. Kang, K.J. Jeong, J. Lee, J.W. Han, W.S. Choi, Y.K. Kim, J. Kang, C.G. Park, H.Y. Lee, Norepinephrine induces VEGF expression and angiogenesis by a hypoxia-inducible factor-1alpha protein-dependent mechanism, Int J Cancer 128(10) (2011) 2306-2316.

[9] B. Russo, M. Menduni, P. Borboni, F. Picconi, S. Frontoni, Autonomic nervous system in obesity and insulin-resistance-the complex interplay between leptin and central nervous System, Int J Mol Sci 22(10) (2021) 5187.

[10] J.W. Jocken, E.E. Blaak, Catecholamine-induced lipolysis in adipose tissue and skeletal muscle in obesity, Physiol & Behav 94(2) (2008) 219-230.

[11] L. Millet, P. Barbe, M. Lafontan, M. Berlan, J. Galitzky, Catecholamine effects on lipolysis and blood flow in human abdominal and femoral adipose tissue, J Appl Physiol 85(1) (1998) 181-188.

[12] H. Yamashita, N. Sato, T. Kizaki, S. Oh-ishi, M. Segawa, D. Saitoh, Y. Ohira, H. Ohno, Norepinephrine stimulates the expression of fibroblast growth factor 2 in rat brown adipocyte primary culture, Cell Growth Differ 6(11) (1995) 1457-1462.

[13] J.M. Fredriksson, J.M. Lindquist, G.E. Bronnikov, J. Nedergaard, Norepinephrine induces vascular endothelial growth factor gene expression in brown adipocytes through a beta -adrenoreceptor/cAMP/protein kinase A pathway involving Src but independently of Erk1/2, J Biol Chem 275(18) (2000) 13802-13811.

[14] C. Tonello, A. Giordano, V. Cozzi, S. Cinti, M.J. Stock, M.O. Carruba, E. Nisoli, Role of sympathetic activity in controlling the expression of vascular endothelial growth factor in brown fat cells of lean and genetically obese rats, FEBS Lett 442(2-3) (1999) 167-172.

[15] A. Asano, M. Morimatsu, H. Nikami, T. Yoshida, M. Saito, Adrenergic activation of vascular endothelial growth factor mRNA expression in rat brown adipose tissue: implication in cold-induced angiogenesis, Biochem J 328 (Pt 1) (1997) 179-183.

[16] P. Balakumar, A. Alqahtani, N.A. Khan, T. Alqahtani, T. A, G. Jagadeesh, The physiologic and physiopathologic roles of perivascular adipose tissue and its interactions with blood vessels and the renin-angiotensin system, Pharmacol Res 173 (2021) 105890.

[17] V. Mohamed-Ali, L. Flower, J. Sethi, G. Hotamisligil, R. Gray, S.E. Humphries, D.A. York, J. Pinkney, beta-Adrenergic regulation of IL-6 release from adipose tissue: in vivo and in vitro studies, J Clin Endocrinol Metab 86(12) (2001) 5864-5869.

[18] R. Gao, X. Peng, C. Perry, H. Sun, A. Ntokou, C. Ryu, J.L. Gomez, B.C. Reeves, A. Walia, N. Kaminski, N. Neumark, G. Ishikawa, K.E. Black, L.P. Hariri, M.W. Moore, M. Gulati, R.J. Homer, D.M. Greif, H.K. Eltzschig, E.L. Herzog, Macrophage-derived netrin-1 drives adrenergic nerve-associated lung fibrosis, J Clin Invest 131(1) (2021) e136542.

[19] J. Lyu, M. Wang, X. Kang, H. Xu, Z. Cao, T. Yu, K. Huang, J. Wu, X. Wei, Q. Lei, Macrophage-mediated regulation of catecholamines in sympathetic neural remodeling after myocardial infarction, Basic Res Cardiol 115(5) (2020) 56.

623 [20] J.A. Oben, T. Roskams, S. Yang, H. Lin, N. Sinelli, Z. Li, M. Torbenson, S.A. Thomas,
624 A.M. Diehl, Norepinephrine induces hepatic fibrogenesis in leptin deficient ob/ob mice,
625 Biochem Biophys Res Commun 308(2) (2003) 284-292.
626 [21] B. Rassler, G. Marx, K. Schierle, H.G. Zimmer, Catecholamines can Induce pulmonary
627 remodeling in rats, Cell Physiol Biochem. 30(5) (2012) 1134-1147.
628 [22] A. Divoux, J. Tordjman, D. Lacasa, N. Veyrie, D. Hugol, A. Aissat, A. Basdevant, M.
629 Guerre-Millo, C. Poitou, J.D. Zucker, P. Bedossa, K. Clement, Fibrosis in human adipose
630 tissue: composition, distribution, and link with lipid metabolism and fat mass loss, Diabetes
631 59(11) (2010) 2817-2825.
632 [23] G.J. Hausman, Cytochemistry for lectins, actin, nucleotide tetrazolium reductases and
633 several phosphatases in the porcine semitendinosus muscle: vascular development in young
634 pigs, J Anim Sci 67(5) (1989) 1375-1386.
635 [24] S. Matsumoto, K. Morikawa, M. Yanagida, Light microscopic structure of DNA in
636 solution studied by the 4',6-diamidino-2-phenylindole staining method, J Mol Biol 152(2)
637 (1981) 501-516.
638 [25] O. Gealekman, N. Guseva, C. Hartigan, S. Apotheker, M. Gorgoglione, K. Gurav, K.V.
639 Tran, J. Straubhaar, S. Nicoloro, M.P. Czech, M. Thompson, R.A. Perugini, S. Corvera,
640 Depot-specific differences and insufficient subcutaneous adipose tissue angiogenesis in
641 human obesity, Circulation 123(2) (2011) 186-194.
642 [26] P. Chomczynski, N. Sacchi, Single-step method of RNA isolation by acid guanidinium
643 thiocyanate-phenol-chloroform extraction, Anal Biochem 162(1) (1987) 156-159.
644 [27] A. Chen, I. Cuevas, P.A. Kenny, H. Miyake, K. Mace, C. Ghajar, A. Boudreau, M.J.
645 Bissell, N. Boudreau, Endothelial cell migration and vascular endothelial growth factor
646 expression are the result of loss of breast tissue polarity, Cancer Res 69(16) (2009) 6721-9.

[28] C.F. Wenceslau, C.G. McCarthy, S. Earley, S.K. England, J.A. Filosa, S. Goulopoulou, D.D. Gutterman, B.E. Isakson, N.L. Kanagy, L.A. Martinez-Lemus, S.K. Sonkusare, P. Thakore, A.J. Trask, S.W. Watts, R.C. Webb, Guidelines for the measurement of vascular function and structure in isolated arteries and veins, Am J Physiol Heart Circ Physiol 321(1) (2021) H77-h111.

[29] M.J. Mulvany, W. Halpern, Contractile properties of small arterial resistance vessels in spontaneously hypertensive and normotensive rats, Circ Res 41(1) (1977) 19-26.

[30] W.T. Friedewald, R.I. Levy, D.S. Fredrickson, Estimation of the concentration of low-density lipoprotein cholesterol in plasma, without use of the preparative ultracentrifuge, Clin Chem 18(6) (1972) 499-502.

[31] D.R. Matthews, J.P. Hosker, A.S. Rudenski, B.A. Naylor, D.F. Treacher, R.C. Turner, Homeostasis model assessment: insulin resistance and beta-cell function from fasting plasma glucose and insulin concentrations in man, Diabetologia 28(7) (1985) 412-419.

[32] S. Rajsheker, D. Manka, A.L. Blomkalns, T.K. Chatterjee, L.L. Stoll, N.L. Weintraub, Crosstalk between perivascular adipose tissue and blood vessels, Curr Opin Pharmacol 10(2) (2010) 191-196.

[33] J.R. Su, Z.H. Lu, Y. Su, N. Zhao, C.L. Dong, L. Sun, S.F. Zhao, Y. Li, Relationship of serum adiponectin levels and metformin therapy in patients with type 2 diabetes, Horm Metab Res 48(2) (2016) 92-98.

[34] R. Kvetnansky, J. Ukropec, M. Laukova, B. Manz, K. Pacak, P. Vargovic, Stress stimulates production of catecholamines in rat adipocytes, Cell Mol Neurobiol 32(5) (2012) 801-813.

[35] P. Vargovic, J. Ukropec, M. Laukova, S. Cleary, B. Manz, K. Pacak, R. Kvetnansky, Adipocytes as a new source of catecholamine production, FEBS Lett 585(14) (2011) 2279-2284.

672 [36] P. Vargovic, M. Laukova, J. Ukropec, G. Manz, R. Kvetnansky, Lipopolysaccharide
673 induces catecholamine production in mesenteric adipose tissue of rats previously exposed to
674 immobilization stress, Stress 19(4) (2016) 439-447.
675 [37] K.D. Nguyen, Y. Qiu, X. Cui, Y.P. Goh, J. Mwangi, T. David, L. Mukundan, F.
676 Brombacher, R.M. Locksley, A. Chawla, Alternatively activated macrophages produce
677 catecholamines to sustain adaptive thermogenesis, Nature 480(7375) (2011) 104-108.
678 [38] P. Vargovic, G. Manz, R. Kvetnansky, Continuous cold exposure induces an anti-
679 inflammatory response in mesenteric adipose tissue associated with catecholamine
680 production and thermogenin expression in rats, Endocr Regul 50(3) (2016) 137-144.
681 [39] A. Gomes, F. Leite, L. Ribeiro, Adipocytes and macrophages secretomes coregulate
682 catecholamine-synthesizing enzymes, Int J Med Sci 18(3) (2021) 582-592.
683 [40] I. Elias, S. Franckhauser, T. Ferre, L. Vila, S. Tafuro, S. Munoz, C. Roca, D. Ramos, A.
684 Pujol, E. Riu, J. Ruberte, F. Bosch, Adipose tissue overexpression of vascular endothelial
685 growth factor protects against diet-induced obesity and insulin resistance, Diabetes 61(7)
686 (2012) 1801-1813.
687 [41] K. Sun, I. Wernstedt Asterholm, C.M. Kusminski, A.C. Bueno, Z.V. Wang, J.W. Pollard,
688 R.A. Brekken, P.E. Scherer, Dichotomous effects of VEGF-A on adipose tissue dysfunction,
689 PNAS 109(15) (2012) 5874-5879.
690 [42] T. Hunyenyiwa, K. Hendee, K. Matus, P. Kyi, T. Mammoto, A. Mammoto, Obesity
691 inhibits angiogenesis through TWIST1-SLIT2 signaling, Front Cell Dev Biol 9 (2021)
692 693410-693410.
693 [43] A. Villaret, J. Galitzky, P. Decaunes, D. Esteve, M.A. Marques, C. Sengenes, P.
694 Chiotasso, T. Tchkonia, M. Lafontan, J.L. Kirkland, A. Bouloumie, Adipose tissue
695 endothelial cells from obese human subjects: differences among depots in angiogenic,

696 metabolic, and inflammatory gene expression and cellular senescence, Diabetes 59(11) (2010)
697 2755-2763.
698 [44] M. Longo, F. Zatterale, J. Naderi, L. Parrillo, P. Formisano, G.A. Raciti, F. Beguinot, C.
699 Miele, Adipose tissue dysfunction as determinant of obesity-associated metabolic
700 complications, Int J Mol Sci 20(9) (2019) 2358.
701 [45] A.K. Ziegler, A. Damgaard, A.L. Mackey, P. Schjerling, P. Magnusson, A.T. Olesen, M.
702 Kjaer, C. Scheele, An anti-inflammatory phenotype in visceral adipose tissue of old lean mice,
703 augmented by exercise, Sci Rep 9(1) (2019) 12069.
704 [46] M.G. Farb, L. Ganley-Leal, M. Mott, Y. Liang, B. Ercan, M.E. Widlansky, S.J. Bigornia,
705 A.J. Fiscale, C.M. Apovian, B. Carmine, D.T. Hess, J.A. Vita, N. Gokce, Arteriolar function
706 in visceral adipose tissue is impaired in human obesity, Arterioscler Thromb Vasc Biol 32(2)
707 (2012) 467-473.
708 [47] A. Raees, A. Bakhamis, V. Mohamed-Ali, M. Bashah, M. Al-Jaber, D. Abraham, L.H.
709 Clapp, N.N. Orie, Altered cyclooxygenase-1 and enhanced thromboxane receptor activities
710 underlie attenuated endothelial dilatory capacity of omental arteries in obesity, Life Sci 239
711 (2019) 117039.
712 [48] H.J. Lee, H. Shi, H.S. Brönneke, B.Y. Jin, S.H. Choi, R.J. Seeley, D.H. Kim, Vascular
713 reactivity contributes to adipose tissue remodeling in obesity, J Endocrinol 251(3) (2021)
714 195-206.
715 [49] M.M. Ali, C. Hassan, M. Masrur, F.M. Bianco, D. Naquiallah, I. Mirza, P. Frederick,
716 E.T. Fernandes, C.P. Giulianotti, A. Gangemi, S.A. Phillips, A.M. Mahmoud, Adipose tissue
717 hypoxia correlates with adipokine hypomethylation and vascular dysfunction, Biomedicines
718 9(8) (2021) 1034.
719 [50] P.Z. Costa, R. Soares, Neovascularization in diabetes and its complications. Unraveling
720 the angiogenic paradox, Life Sci 92(22) (2013) 1037-1045.

[51] N. Ball, J.L. Danks, S. Dorudi, P.A. Nasmyth, Desensitization by noradrenaline of responses to stimulation of pre- and postsynaptic adrenoceptors, Br J Pharmacol 76(1) (1982) 201-210.

[52] W. Chen, J.Y. Sang, D.J. Liu, J. Qin, Y.M. Huo, J. Xu, Z.Y. Wu, Desensitization of G-protein-coupled receptors induces vascular hypocontractility in response to norepinephrine in the mesenteric arteries of cirrhotic patients and rats, Hepatobiliary Pancreat Dis Int 12(3) (2013) 295-304.

[53] P.K. Chaudhary, S. Kim, S. Kim, The predominant role of arrestin3 in general GPCR desensitization in platelets, J Clin Med 10(20) (2021) 4743.

[54] L. Tobin, L. Simonsen, H. Galbo, J. Bulow, Vascular and metabolic effects of adrenaline in adipose tissue in type 2 diabetes, Nutr Diabetes 2 (2012) e46.

[55] H.B. Hubert, M. Feinleib, P.M. Mcnamara, W.P. Castelli, Obesity as an Independent Risk Factor for Cardiovascular-Disease - a 26-Year Follow-up of Participants in the Framingham Heart-Study, Circulation 67(5) (1983) 968-977.

[56] B. Larsson, K. Svardsudd, L. Welin, L. Wilhelmsen, P. Bjorntorp, G. Tibblin, Abdominal adipose tissue distribution, obesity, and risk of cardiovascular disease and death: 13 year follow up of participants in the study of men born in 1913, Br Med J 288(6428) (1984) 1401-1404.

[57] J.A. Kim, M. Montagnani, K.K. Koh, M.J. Quon, Reciprocal relationships between insulin resistance and endothelial dysfunction - Molecular and pathophysiological mechanisms, Circulation 113(15) (2006) 1888-1904.

[58] N. Chaihongsa, P. Maneesai, W. Sangartit, P. Potue, S. Bunbupha, P. Pakdeechote, Galangin alleviates vascular dysfunction and remodelling through modulation of the TNF-R1, p-NF-κB and VCAM-1 pathways in hypertensive rats, Life Sci 285 (2021) 119965.

745 [59] W.C. Tang, Y.W. Chang, M. Che, M.H. Wang, K.K. Lai, P.T. Fueger, W. Huang, S.B.
746 Lin, K.K.Y. Lai, Thioacetamide-induced norepinephrine production by hepatocytes is
747 associated with hepatic stellate cell activation and liver fibrosis, Curr Mol Pharmacol (2021)
748 E-pub Ahead of Print.
749 [60] J. Diez, A. Panizo, M.J. Gil, I. Monreal, M. Hernandez, J. Pardo Mindan, Serum markers
750 of collagen type I metabolism in spontaneously hypertensive rats: relation to myocardial
751 fibrosis, Circulation 93(5) (1996) 1026-1032.
752 [61] C. Laviades, N. Varo, J. Fernandez, G. Mayor, M.J. Gil, I. Monreal, J. Diez,
753 Abnormalities of the extracellular degradation of collagen type I in essential hypertension,
754 Circulation 98(6) (1998) 535-540.
755 [62] C. Pellet-Many, P. Frankel, H. Jia, I. Zachary, Neuropilins: structure, function and role
756 in disease, Biochem J 411(2) (2008) 211-226.

11 Supplementary Figures

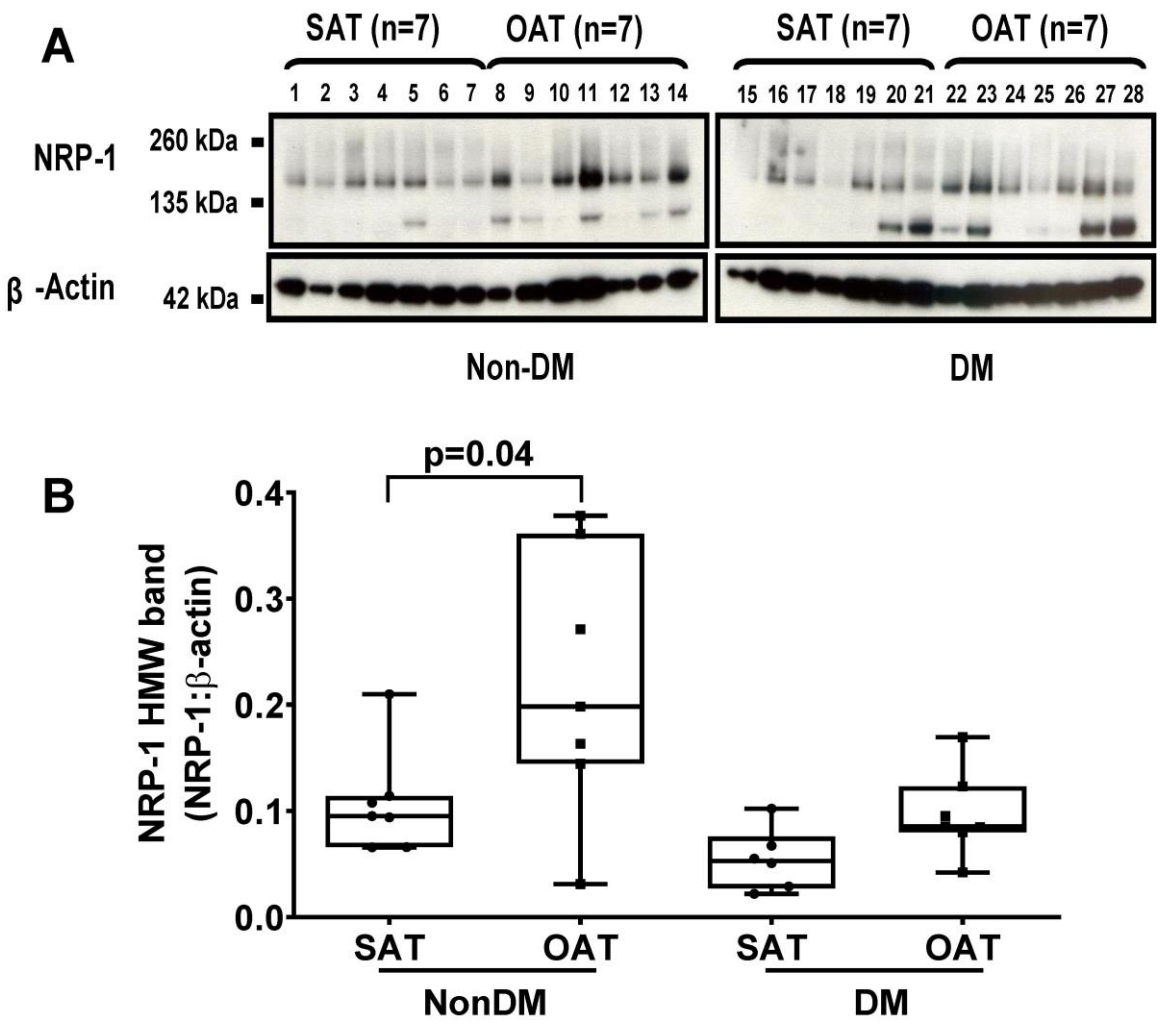

Supplementary Figure 1 Depot- and diabetes-specific differences in NRP-1 protein expression of AT

(A) *Two isoforms of NRP-1 were found in human AT. Overall, the expression of the non-modified NRP1 band (~130 kDa) was relatively lower compared with the higher molecular weight band (>200 kDa), and was up-regulated in the diabetic compared to non-diabetic group, which probably represents glycosylated NRP1 [62]. Furthermore, in the non-diabetic group, the protein expression of the non-modified NRP1 bands were observed in OAT of more patients (n=5 out of 7) than SAT (n=1 out of 7), while NRP-1 with higher molecular weight was more highly expressed in OAT compared to SAT. However, no such depot-*

specific difference was found in the diabetic group. ***(B)*** *Data was analysed by Image J and expressed as grey density ratio between high molecular weight NRP-1 and β-actin.*

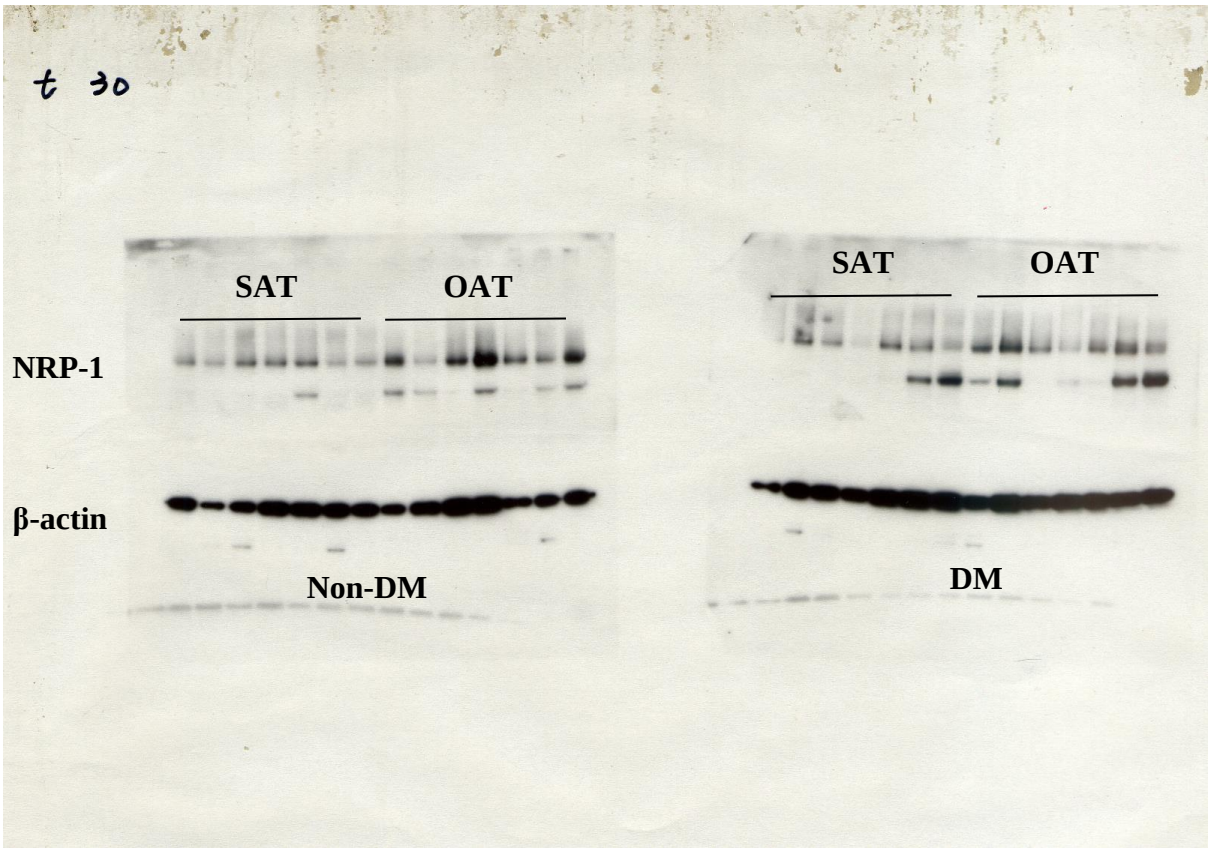

Supplementary Figure 2 Original western blot slide